

# ViFP: A Framework for Visual False Positive Detection to Enhance Reasoning Reliability in VLMs

Ben Zhang, Lulu Yu, Lei Gao, Quanjiang Guo, Jing Liu, Hui Gao

**Abstract**—During reasoning in vision-language models (VLMs), false positive (FP) reasoning occurs when a model produces the correct answer but follows an incorrect reasoning path, resulting in undermined reasoning reliability. Existing approaches mainly rely on prompt engineering, knowledge distillation or reinforcement learning to improve reasoning reliability, both of which require large amounts of high-quality data and thus limit practical applicability. Few approaches have focused on directly detecting and correcting FPs. To address these issues, we propose ViFP, a framework for Visual False Positive Detection to Enhance Reasoning Reliability in VLMs. ViFP builds effective reasoning paths through multi-turn QA and dynamically analyzes the consistency of the reasoning path to identify potential FPs. It also introduces a targeted reasoning chain correction mechanism to modify FP reasoning, thereby improving logical consistency and accuracy. Finally, we introduce a reliability evaluation metric—VoC, which integrates answer accuracy and the FP rate, providing a quantitative tool to assess whether a VLM not only answers correctly but also reasons reliably. Our experiments on closed-source VLMs show that ViFP consistently improves performance across three datasets: A-OKVQA, OK-VQA, and FVQA. On A-OKVQA, ViFP improves accuracy by up to 5.4%, surpassing the previous state-of-the-art by 4.3%, and significantly reduces the number of FPs, validating its benefits in enhancing reasoning reliability.

**Index Terms**—Visual Reasoning, Vision-Language Models, False Positive Reasoning, Reasoning Reliability, Reliability Evaluation.

## I. INTRODUCTION

Recent studies have shown that vision-language models (VLMs) achieve outstanding performance on visual question answering (VQA) [1]–[5]. By integrating visual encoders with large language models (LLMs), VLMs jointly encode images and text into a unified vector space. This makes use of the powerful language understanding and generation capabilities of LLMs, while also enabling prompt engineering to generate structured reasoning paths. When the model’s output includes explicit reasoning chains, the phenomenon of false positive (FP) reasoning may emerge. An FP refers to instances where the model produces the correct final answer but follows an incorrect reasoning path [6], as illustrated in Fig. 1. A key cause of FPs lies in the model performing “illusory reasoning”, whereby the reasoning path is not derived through step-by-step deduction, but instead reverse-engineered to justify a

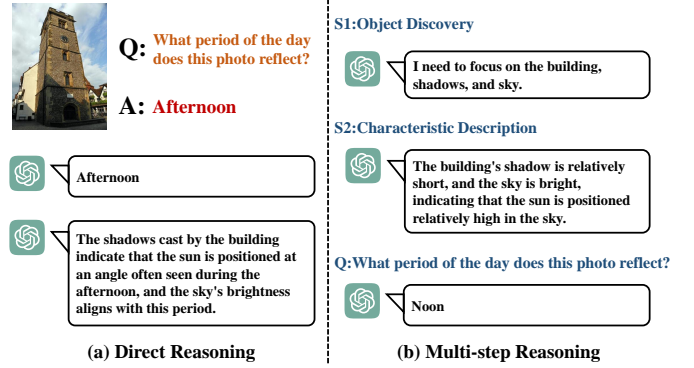


Fig. 1. FP instance in visual reasoning. The VLM follows the same reasoning path twice (sun→building→shadows) but produces different answers (afternoon and noon).

predetermined answer. Therefore, FPs are a critical factor that undermines the reliability of visual reasoning.

To improve reasoning reliability, some existing approaches use Chain-of-Thought (CoT) prompting to guide VLMs in generating explicit reasoning paths that support conclusions [7]–[10]. Rather than explicitly identifying FP, these methods aim to reduce such errors by strengthening the model’s logical reasoning capabilities. CoT decomposes complex questions into simpler sub-questions and forces the generation of intermediate reasoning paths [11]–[13]. Some approaches use a standard template and assign the decomposition task to the VLM. This strategy does not provide any effective reasoning clues or supplementary information. The decomposition process is prone to deviations or errors. Distillation methods typically leverage powerful closed-source VLMs like GPT to generate high-quality training data, which is then used to train a smaller, more resource-efficient model, such as LLaVA-CoT [14], [15]. However, due to the smaller model’s inherent capacity limitations, the distilled model cannot surpass the reasoning capabilities of the original high-performing VLM. While this approach enables computationally efficient, small-scale models to be distilled, it is not suitable for directly improving high-performing VLMs.

The above approaches aim to improve the reliability of reasoning through forward enhancement. However, few approaches address the issue of reverse verification, particularly with regard to detecting and correcting FP. Current FP detection methods fall into two categories: human and model-based [6]. The former is inefficient and lacks scalability, while the latter, although automated, typically relies on high-performance supervisory models. This creates a dilemma: if a superior VLM is needed to judge reasoning validity, it is

Ben Zhang, Lulu Yu, Lei Gao, Quanjiang Guo, and Jing Liu are with the School of Computer Science and Engineering, University of Electronic Science and Technology of China, Chengdu 611731, China (E-mail: zhangben@std.uestc.edu.cn; yululu@std.uestc.edu.cn; leigao@std.uestc.edu.cn; guochance1999@163.com; liuj1017@163.com).

Hui Gao is with the School of Computer Science and Engineering, University of Electronic Science and Technology of China, Chengdu, China and also with Kash Institute of Electronics and Information Industry, Kash 844000, China (E-mail: huigao@uestc.edu.cn).

often more efficient to use that superior VLM for reasoning. Meanwhile, both human and model-based evaluations suffer from inconsistent cognitive standards in FP. Assume a supervisory model to review the reasoning process of the inference model. As shown in the example in Fig. 1, a supervisory model receiving only the direct reasoning (left) might deem it valid (e.g. accepting "reasoning time from sunlight and shadows" as feasible). However, if in reality the model cannot progress from analyzing the lighting to reasoning the time (right), it suggests that the reasoning logic is flawed and should be classified as a FP. This allows users to identify which parts of the VLM's reasoning are unreliable. By designing effective reasoning strategies or fine-tuning the model based on FP instances, the accuracy and reliability of VLM visual reasoning can be improved.

In summary, we propose ViFP, a framework for visual FP detection to enhance reasoning reliability in VLMs. ViFP is compatible with leading closed-source VLMs including GPT-4o, Gemini-2.5, and Grok-4. ViFP employs a prompt-based evaluation to detect FPs by assessing the consistency between direct and multi-step reasoning outputs. Meanwhile, an exclusive correction mechanism has been introduced to optimize multi-step reasoning paths, improving overall reliability in terms of both answer accuracy and reasoning path reliability. ViFP constructs a generalizable sub-question set derived from real-world question-solving logic, and defines the mapping between question types and reasoning chains. This requires the model to perform targeted, multi-step reasoning based on the question type. This design ensures the normativity of the reasoning process, while enabling the model to adapt to complex scenarios by adjusting the reasoning chain flexibly.

Finally, we conducted experiments to evaluate ViFP on three real-world VQA datasets, demonstrating its ability to detect and correct FPs, as well as improve both the reasoning accuracy and reasoning path reliability of base VLMs. The main contributions of our method are as follows:

- We propose ViFP, a fast and lightweight FP self-detection framework that can be seamlessly applied to various VLMs;
- We introduce a visual reasoning optimization method based on feedback from FPs. This enables VLMs to adapt the reasoning chain dynamically, achieving more accurate and reliable reasoning;
- We introduce a novel metric for assessing reasoning reliability — VoC(Value of Correction) and validate it on closed-source VLMs, demonstrating its preliminary feasibility in assessing reasoning reliability.

## II. RELATED WORK

### A. Visual Reasoning in VLMs

VQA tasks require models to possess visual perception, cognitive reasoning, and extensive knowledge resources [16], [17]. With these three objectives in mind, researchers have continually explored more efficient and unified approaches. BLIP-2 introduces a Q-Former module that selectively attends to important regions in the image, enhancing accuracy but increasing hallucinations [1]. MiniCPM and Mini-Monkey

have designed special image patch segmentation strategies and reduced model size for deployment on the device side, resulting in weak multi-step inference capabilities [4], [5]. MoMe, Omni-SMoLA, and VLMO flexibly use Mixture-of-Experts (MoE) to adapt to various tasks and improve generalization, but this increases training costs [18]–[20]. GraphVis and GeReA incorporate external knowledge graphs to assist reasoning and expand the model's knowledge base, but these methods rely on high-quality knowledge bases [21]–[25]. DEDR further employs an iterative knowledge distillation approach over external knowledge bases such as Wikipedia to capture high-quality knowledge and generates answers using the MM-FiD decoder [26]. MM-Reasoner generates detailed image captions and extracts key objects that appear. This information is used to prompt the LLM to dynamically generate relevant knowledge, thereby avoiding reliance on a traditional static knowledge base retrieval [27]. LLMs inherently store vast amounts of knowledge, with larger models offering richer information. Prophet leverages this capability by prompting LLMs to generate auxiliary knowledge, guiding a base VQA model to better identify the correct answer among candidates [28], [29].

### B. Reliable Reasoning in VLMs

The reliability of reasoning has long been a central concern. Existing approaches primarily focus on enhancing the reasoning capabilities of models [7], [8], [10], often through CoT, which encourages the model to output intermediate steps and decompose complex questions into simpler sub-questions [9]. For example, prompting strategies like "Let's think step by step." and LLaVA-CoT assign the task of question decomposition to the powerful VLMs by designing general-purpose question templates. While these approaches promote versatility, they overly rely on the model's inherent reasoning ability and fail to consistently improve the performance of these powerful VLMs [14], [15]. Visual-CoT further builds upon the idea of question decomposition by annotating images with visual highlights of key regions essential for answering, effectively producing explicit visual attention [14].

In addition, some recent works in mathematics and physics domains have attempted to detect FP reasoning by introducing specific benchmarks for FP identification, or by constructing targeted datasets to help models learn reliable reasoning logic [6], [30], [31].

## III. METHODOLOGY

The overall architecture of ViFP is shown in Fig.2. Given an input image question pair, the VLM first generates a direct reasoning result. ViFP then classifies the question and constructs a corresponding reasoning chain composed of a sequence of sub-questions. The VLM sequentially answers the sub-questions, the outputs are used to detect FPs by examining the consistency with the direct reasoning. Finally, the detected FPs are used to discover new question types and optimize reasoning-chain templates, thereby improving the reliability of visual reasoning in VLM.

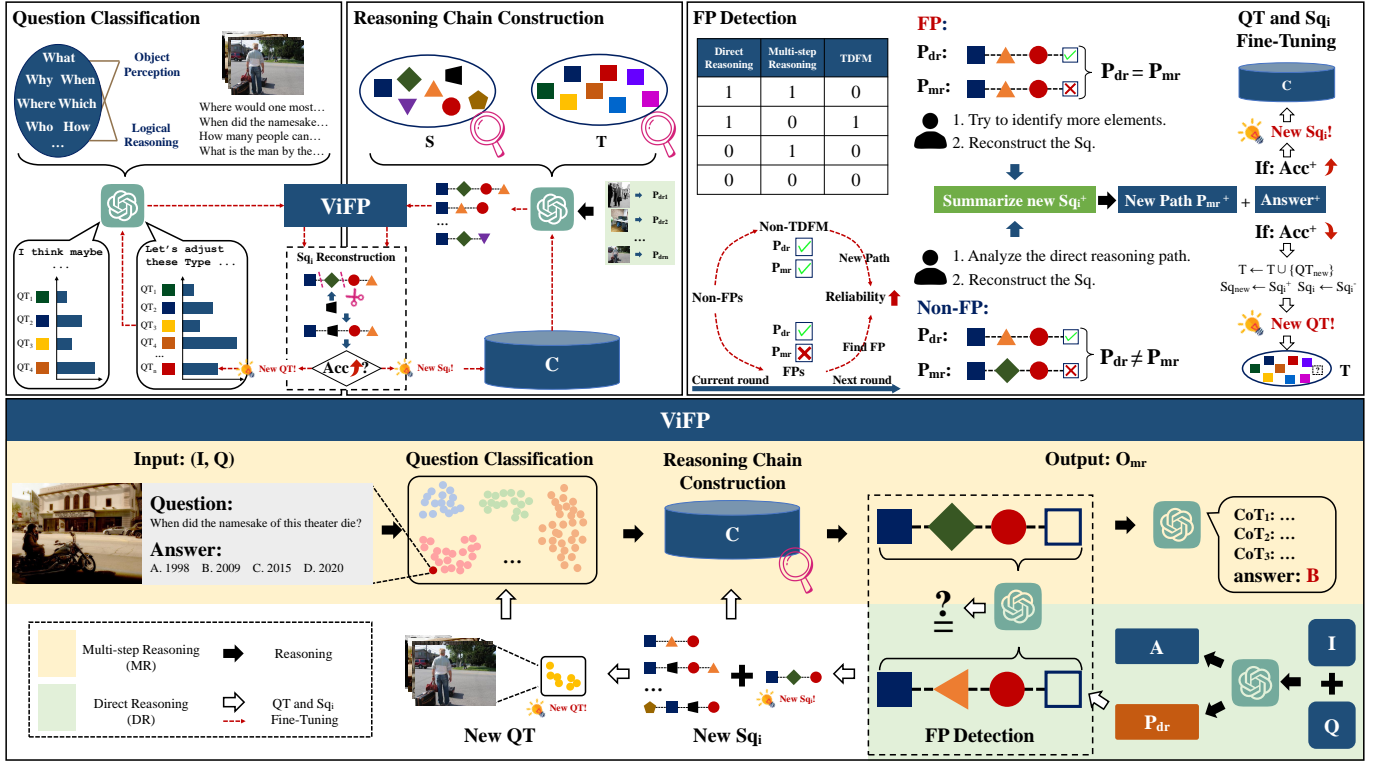


Fig. 2. The overview framework of ViFP. (1) Question Classification: real-world VQA questions are classified along the dimensions of perception and reasoning, forming the initial question types. (2) Reasoning Chain Construction: the VLM summarizes reasoning chain templates for use in multi-step reasoning. (3) FP Detection: detecting FPs by comparing the consistency between direct and multi-step reasoning. (4)  $QT$  and  $Sq_i$  Fine-Tuning: Based on the detected FPs, the VLM refines the question types and the corresponding reasoning chains. (5) ViFP: Given an input (image question pair), ViFP conducts multi-step reasoning and iteratively refines its next reasoning to produce more accurate answers.

### A. Question Classification

The initial question types are generated by the VLM with the following prompt:

User: <Question>... How should real-world VQA questions be classified according to differences in object localization and logical reasoning?  
ASSISTANT: <output>.

The output is a set  $T = \{QT_1, \dots, QT_k\}$ , where the  $i$ -th question type is denoted as  $QT_i$ . “object localization” and “logical reasoning” are included in the prompt as few-shot cues to prevent the VLM from blindly initiating classification. This design can improve the reproducibility of ViFP.

### B. Reasoning Chain Construction

First, the initial sub-question set is generated by the VLM with the following prompt:

User: <Image><Question> Answer the question, provide the reason and the confidence scores for each option as probabilities that sum to 1.  
ASSISTANT: <output>.  
User: <Reason>... Summarize the chain step by step, such as scene description and relationship description...  
ASSISTANT: <output>.

The first output is the direct reasoning result  $O_{dr} = (P_{dr}, A)$ , where  $P$  denotes the reasoning path, the subscript

“dr” stands for direct reasoning, and  $A$  denotes the answer. Meanwhile, each option has a confidence score  $p$  representing the probability of being the correct answer. The second output is a sequence of questions  $Sq = \langle q_1, \dots, q_n \rangle$ , where  $q$  denotes the sub-question.

Based on the reasoning path derived from direct reasoning, the VLM summarizes the reasoning chain template for each type of question by using the following prompt:

User: <Reason>... Analyze the above paths, then select sub-questions from <q>... to construct a reasoning chain for <Type> question.  
ASSISTANT: <output>.

The output is the reasoning chain template  $Sq_i = \{Sq \mid QT_i\}$ , total number is  $k$ .

In the next round of multi-step reasoning,  $Sq_i$  is used as the reasoning chain, the output is  $O_{mr} = (P_{mr}, A)$ , where  $P_{mr}$  is a sequence of QA pairs  $P_{mr} = \langle (q_1, A_1), \dots, (q_n, A_n) \rangle$ , and the subscript “mr” stands for multi-step reasoning.

### C. FP Detection

The error distributions differ between direct reasoning and multi-step reasoning. We define certain instances as TDFM

$$TDFM = \{(P_{dr}, P_{mr}) \mid f(P_{dr}) = A^*, f(P_{mr}) \neq A^*\}, \quad (1)$$

where  $A^*$  denotes the ground truth, TDFMs are used for FP detection. To formally characterize, the visual reasoning process is defined as a mapping function  $f(P) = A$ .

Assume there are  $(P_{dr}, A_{dr})$  and  $(P_{mr}, A_{mr})$ , if  $P_{dr} = P_{mr}$ , but  $A_{dr} \neq A_{mr}$ , it implies that  $f(P) = A_{dr}$  and  $f(P) = A_{mr}$  hold simultaneously, which violates the definition of a function. Therefore, such a mapping function cannot exist, the  $P_{dr}$  is identified as a FP. ViFP modifies its  $Sq$  in order to discover a more reliable path. The prompt used in this part is shown as follows:

```
User: <Image><Question><Path> The above reasoning path
is incorrect. Try to identify more elements in the image
and reconstruct the reasoning chain.
ASSISTANT: <output>.
```

If  $P_{dr} \neq P_{mr}$ , this indicates that  $Sq_i$  changes the reasoning path, and thus  $P_{dr}$  cannot be asserted to be a FP. ViFP then analyzes the original path  $P_{dr}$  and reconstructs  $Sq$ . If the TDFM is converted into a non-TDFM in the next round of reasoning, namely, if  $(P_{dr}^+ = P_{mr}^+) \wedge (A^+ = A^*)$ , then  $P_{dr} \notin \text{FP}$ , where the superscript "+" stands for the next round of reasoning. Otherwise, the instance remains TDFM and is identified as a FP. namely, if  $(P_{dr}^+ = P_{mr}^+) \wedge (A^+ \neq A^*)$ , then  $P_{dr} \in \text{FP}$ . The prompt used in this part is shown as follows:

```
User: <Image><Question><Path> The above reasoning path
is incorrect. Reconstruct the reasoning chain to align
with the original path <Reason>.
ASSISTANT: <output>.
```

The output of the above two parts is a new reasoning chain  $Sq$ , which is used to summarize the new  $Sq_i^+$ .

#### D. $QT$ and $Sq_i$ Fine-tuning

ViFP is a training-free method but requires fine-tuning of  $QT$  and  $Sq_i$ . Based on the new reasoning chain  $Sq$ , the prompt used to summarize  $Sq_i^+$  is shown as follows:

```
User: <Path>... Summarize these paths into a reasoning
chain by selecting sub-questions from <q>....
Generate <n> different candidate reasoning chains.
ASSISTANT: <output>...
```

The output consists of  $n$  candidate reasoning chains generated by the VLM, and ViFP evaluates them using information gain (IG) to enhance the adaptability of reasoning templates:

$$IG(Q | Sq_{ij}) = H(Q) - H(Q | A_j), \quad (2)$$

where  $H(Q)$  stands for the uncertainty (entropy) of the answer to the question  $Q$ , the subscript "j" stands for the j-th candidate reasoning chain, and  $H(Q | A_j)$  denotes the conditional entropy of answering  $Q$  given the answers  $A_j$ . The calculation formula for  $H$  is:

$$H(Q) = - \sum_{i=1}^n p(a) \log p(a), \quad (3)$$

where  $p(a)$  denotes the confidence score of option  $a$ .

ViFP selects the candidate reasoning chain that maximizes the IG as the final  $Sq_i^+$ :

$$Sq_i^+ = \arg \max_{Sq_{ij}} \frac{1}{n} IG_{total}(Q | Sq_{ij}), \quad (4)$$

In the next round of reasoning, VLM generates the new output  $O_{mr}^+$  based on the  $Sq_i^+$ . When  $QT = QT_i$ , if the corresponding reasoning accuracy increases, then  $Sq_i \leftarrow Sq_i^+$ . If the reasoning accuracy decreases, a new question type  $QT_{new}$  is created and  $Sq_{new} \leftarrow Sq_i^+$ , while  $Sq_i$  reverts to  $Sq_i^-$  (the superscript "-" stands for the previous round of reasoning).

#### E. Fine-tuning Termination and Outcome

If  $QT_{new}$  is generated, all instances are reclassified. If the new type covers at least 50% of the incorrect instances from the previous round, it is retained. Otherwise, it is deleted. When ViFP no longer generates any  $QT_{new}$ , the fine-tuning process stops.

As shown in Tables I, II and III, after multiple rounds of fine-tuning, ViFP generated 10 sub-questions, 11 question types, each type containing 2 to 4 sub-questions. In Table III, the confidence is calculated as:

$$\text{confidence} = \frac{\text{support}}{\phi}, \quad (5)$$

where support denotes the number of instances for which the final answer is correct when the VLM follows  $Sq_i$ , and  $\phi$  stands for the number of questions whose type is  $QT_i$ .

## IV. EXPERIMENTS

### A. Dataset

We conduct our experiments on three VQA datasets: A-OKVQA [32], OK-VQA [33] and FVQA [34]—to evaluate ViFP's generalizability on real-world VQA tasks. A-OKVQA provides multiple-choice options, while OK-VQA and FVQA are open-ended, with each question having multiple human-annotated answers. The A-OKVQA training set contains 17,056 instances, 1,145 instances in the validation set, and 6,702 instances in the test set. The OK-VQA test set contains 5,046 instances, and the FVQA test set contains 2,778 instances. We fine-tune ViFP on the A-OKVQA training set, as this dataset provides answer options. This setup facilitates the filtering of TDFMs and the subsequent detection of FPs.

### B. Baseline

We first evaluated the performance of ViFP on three mainstream closed-source VLMs: GPT-4o, Gemini-2.5-flash and Grok-4 in order to evaluate ViFP's cross-model performance. Subsequently, we conducted a comparative analysis with 7 open-source state-of-the-art trainable models: PromptCap [35], ZS-F-VQA [36], DEDR [26], MM-Reasoner [27], SMoLA-PaLI-X [19] MiniCPM-V-2.6 [4] and Prophet++ [29]. To intuitively evaluate the effectiveness of the reasoning chain provided by ViFP, we compare ViFP with two CoT approaches—"Let's think step by step" and LLaVA-CoT in the ablation study.

TABLE I  
DESCRIPTION OF QUESTION TYPES

Question Type	Description
Object Localization and Recognition (OLR)	Locate the object in the image and identify what it is.
Temporal Reasoning (TR)	Determine the season, era, or time of day depicted in the image.
Geolocation (GL)	Identify the environment, location, region, or country shown in the image.
Analogical Reasoning (AR)	Compare the consistency between the options and the object in the question.
Functional Reasoning (FR)	Locate and recognize the object, then analyze its function or use.
Intentional Reasoning (IR)	Interpret the object's next action or determine whether a certain action can be performed.
State Perception (SP)	Select the most appropriate adjective from the options to describe the object's state.
Causal Reasoning (CR)	Explain phenomena or infer causality.
Action Perception (AP)	Understand and analyze the actions of objects in the image.
Spatial Relationship (SR)	Judge positional relationships and estimate distances between objects.
Commonsense Reasoning (COR)	Apply real-world commonsense knowledge to interpret the object's behavior.

TABLE II  
DESCRIPTION OF SUB-QUESTIONS

Sub-question	Description
Object Discovery (od)	How many objects do you need to focus on according to the image and question?
Existence Verification (ev)	Do these objects exist in the image?
Object Localization (ol)	Briefly describe their/its location based on the image.
Characteristic Description (cd)	Briefly describe their/its characteristics based on the image.
Scene Description (sd)	Briefly describe the scene based on the image.
Relationship Description (rd)	Briefly describe their relationships based on the image.
Knowledge Retrieval (kr)	Do you need any knowledge to answer this question?
Spatial Relationships Description (srd)	Briefly describe their spatial relationships based on the image.
Temporal Information Discovery (tid)	Is there any object in the image that indicates the time?
Spatial Information Discovery (sid)	Is there any object in the image that indicates the location?

TABLE III  
REASONING CHAIN

Question Type	Reasoning Chain	Confidence
OLR	od → ev → ol	0.908
TR	tid → od → cd	0.895
GL	sid → od → kr	0.960
AR	od → cd → sd	0.920
FR	od → sd	0.916
IR	od → rd → sd	0.896
SP	od → cd	0.742
CR	od → sd → kr	0.957
AP	od → ol → cd → sd	0.865
SR	od → ol → rd	0.750
COR	od → ol → cd → kr	0.783

### C. Implementation Detail

GPT-4o were used to fine-tune ViFP on the A-OKVQA's training set. We classified all instances into four initial question types and sampled 2,000 instances from the training set. These instances were used by the VLM to generate and refine  $QT_i$ ,  $Sq_i$  and so on. During the process, the numbers of  $QT$  were 4, 6, 9, 11, 11, while the accuracy plateaued at 90.7%, after which the fine-tuning process was terminated.

All experiments were conducted on a Linux workstation equipped with a single NVIDIA A800 GPU(80 GB) and Python 3.10. The fine-tuning process on the training set took approximately 24 hours. The total cost was estimated to be under \$ 75 for fine-tuning and under \$100 in total (including fine-tuning and evaluation).

### D. Value of FP Correction

The Value of FP Correction(VoC) is a novel metric that quantifies how FP correction enhances both reasoning accuracy and reliability in ViFP. Existing VQA evaluation metrics mainly focus on accuracy, which may overlook instances of hallucinated or flawed reasoning paths that lead to correct answers.

Unlike conventional accuracy or path matching metrics, VoC integrates three essential components: (1) The improvement in accuracy achieved through multi-step reasoning; (2) The absolute accuracy of reasoning; (3) The capacity to reduce FPs is indirectly estimated via the true negative (TN) rate, which ensures that fewer FPs lead to a higher VoC.

VoC is defined as

$$\text{VoC} = (P - Q) \cdot P \cdot \left( \frac{TN}{FP + TN} \right), \quad (6)$$

where  $P$  and  $Q$  denote the accuracies of multi-step and direct reasoning, respectively,  $FP$  and  $TN$  denote the counts of false positives and true negatives. The final term represents the TN rate, namely the proportion of negative instances correctly predicted as negative.

The partial derivative of VoC with respect to  $P$  is:

$$\frac{\partial \text{VoC}}{\partial P} = (2P - Q) \cdot \left( \frac{TN}{FP + TN} \right) \quad (7)$$

Note that in the region where  $P > \frac{Q}{2}$ , VoC increases with  $P$ . However, when  $P < \frac{Q}{2}$ , VoC becomes negative, indicating that the introduction of new reasoning chain reduces the reasoning reliability. Therefore, in the desirable region where  $P > \frac{Q}{2}$ ,

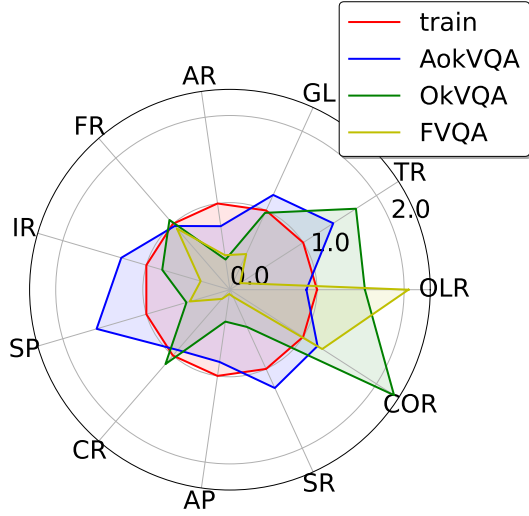


Fig. 3. Data distribution of question types on datasets

a higher VoC value reflects a greater benefit from multi-step reasoning.

The partial derivative of VoC with respect to  $FP$  is:

$$\frac{\partial \text{VoC}}{\partial FP} = \frac{(Q - P) \cdot P \cdot TN}{(FP + TN)^2} \quad (8)$$

Note that in the region where  $P > Q$ , VoC increases as the number of FPs decreases, highlighting the importance of minimizing FPs in improving reasoning reliability.

#### E. Evaluation Strategy

(1) **Generalizability** is evaluated by measuring the difficulty consistency score of each question type across multiple real-world VQA datasets.

$E_{QT_i, D_j}^{(m)}$  denotes the number of incorrect answer instances of type  $QT_i$  made by VLM  $m$  on dataset  $D_j$ ,  $E_{D_j}^{(m)}$  denotes the total number of incorrect answer instances,  $N_{QT_i, D_j}$  denotes the total number of questions of type  $QT_i$  in  $D_j$ , with  $N_{D_j}$  representing the total number of all questions in  $D_j$ .

The relative difficulty of type  $QT_i$  on dataset  $D_j$  for VLM  $m$  is defined as the difference between its error proportion and its occurrence proportion:

$$\text{Dif}_{QT_i, D_j}^{(m)} = \frac{E_{QT_i, D_j}^{(m)}}{E_{D_j}^{(m)}} - \frac{N_{QT_i, D_j}}{N_{D_j}}. \quad (9)$$

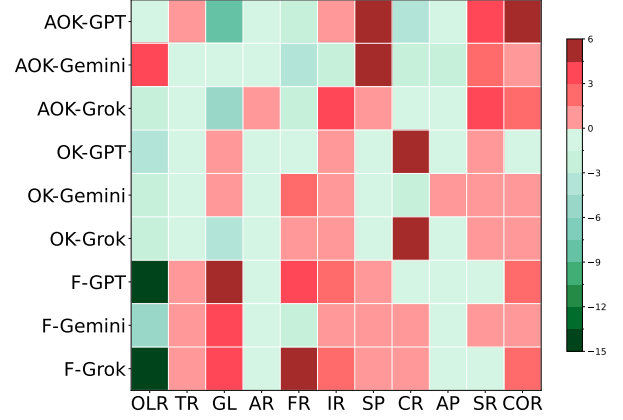


Fig. 4. Difficulty of different question types on datasets

The dataset-level difficulty of question type  $QT_i$  is computed by averaging across all  $M$  VLMs (here  $M = 3$ ):

$$\text{Dif}(QT_i, D_j) = \frac{1}{M} \sum_{m=1}^M \text{Dif}_{QT_i, D_j}^{(m)}. \quad (10)$$

For each  $QT$ ,  $N$  datasets correspond to  $N$  difficulty scores. We then measure the difficulty consistency score  $V(QT_i)$ :

$$V(QT_i) = \frac{1}{N} \sum_{i=1}^N (\text{Dif}(QT_i, D_j) - \overline{\text{Dif}}(QT_i))^2, \quad (11)$$

where the mean difficulty across datasets is

$$\overline{\text{Dif}}(QT_i) = \frac{1}{N} \sum_{i=1}^N \text{Dif}(QT_i, D_j). \quad (12)$$

A smaller  $V(QT_i)$  indicates that the type  $QT_i$  exhibits similar difficulty levels across different datasets, and the performance of ViFP does not drop sharply when applied to these datasets.

(2) **Reasoning accuracy** is assessed on three real-world VQA datasets. A-OKVQA provides four options with only one correct answer. The standard accuracy is adopted as the evaluation metric. OK-VQA and FVQA are open-ended, the top-k matching metric is used as the evaluation metric: the VLM outputs multiple candidate answers, and Top-1 is defined as the probability that the first candidate matches the ground truth. Top-3 is defined as the probability that the ground truth appears among the top three candidates. In order to align with baselines, FVQA is evaluated using both Top-1 and Top-3, whereas OK-VQA only uses Top-1.

TABLE IV  
DIFFICULTY AND CONSISTENCY SCORE  $V(t)$

	OLR	TR	GL	AR	FR	IR	SP	CR	AP	SR	COR
$\text{Dif}(QT_i, D_{A-OKVQA})$	0.53	-0.33	-4.82	0.17	-0.90	1.79	3.30	-1.11	-1.41	3.44	2.44
$\text{Dif}(QT_i, D_{OK-VQA})$	-2.36	-0.24	-0.11	-0.13	0.52	0.56	-0.15	0.68	-0.11	0.15	-0.28
$\text{Dif}(QT_i, D_{FVQA})$	-10.93	0.42	4.01	-0.39	2.67	1.76	0.32	0.09	-0.06	0.00	2.60
$\overline{\text{Dif}}(QT_i)$	-4.26	-0.05	-0.32	-0.11	0.05	1.14	1.16	-0.11	-0.53	1.20	1.59
$V(QT_i)$	23.68	<b>0.11</b>	11.99	<b>0.05</b>	5.52	<b>0.14</b>	<b>2.83</b>	<b>3.32</b>	<b>0.39</b>	<b>2.54</b>	<b>1.55</b>



(3) **Reasoning reliability** is evaluated using three indicators: VoC, FP, and TDFM counts. FP and TDFM counts track the reduction of FP instances and quantify the contribution of newly generated reasoning chains by ViFP to improvements in accuracy.

TABLE V  
COMPARISON BETWEEN ViFP-BASED VLMS AND TRAINABLE MODELS.

Model	A-OKVQA	OK-VQA	FVQA <sub>Top-1</sub>	FVQA <sub>Top-3</sub>
<b>Trainable</b>				
PromptCap	73.2	60.4	-	-
ZS-F-VQA	-	-	58.3	75.2
DEDR	-	51.0	61.8	-
MM-Reasoner	-	60.8	61.1	-
SMoLA-PaLI-X	84.1	62.4	-	-
MiniCPM-V-2.6	86.4	-	-	-
Prophet++	87.7	<b>65.7</b>	-	-
<b>Train-free</b>				
Grok-4	78.1	42.3	64.4	69.2
Gemini-2.5	86.6	46.3	64.8	<b>75.2</b>
GPT-4o	88.8	49.0	69.6	71.7
Grok-4+ViFP	80.0	48.2	66.9	70.4
Gemini-2.5+ViFP	<b>92.0</b>	40.9	61.9	66.3
GPT-4o+ViFP	90.7	55.2	<b>70.3</b>	73.8

#### F. Data distribution

As shown in Fig. 3, we first summarize the distribution of different question types across the three datasets. Second, we compute the relative difficulty and difficulty consistency  $V$  of each question type. As shown in Fig. 4 and Table IV, Eight question types exhibit a relatively low  $V(QT_i)$  value (below 3.5). Only OLR, GL and FR show slightly higher  $V(QT_i)$ , which should be given more attention in ViFP's applications. However, as their  $Dif$  values are relatively low, they don't significantly affect the generalizability of ViFP. As shown in Table V, this is further corroborated by the fact that the accuracy of most VLM+ViFP combinations improves accordingly.

Based on the above information, we can identify which question types the VLM handles more effectively, providing useful guidance for further refining ViFP. Furthermore, these findings also offer recommendations for applying closed-source VLMs and for performing targeted supervised fine-tuning. First, the data distribution for the validation set of A-OKVQA is most similar to the training set, and SP, SR, and COR are relatively difficult, making them key areas to focus on in the next reasoning (refine  $QT$  and  $Sq_i$ ). Grok is more proficient at answering these questions. OK-VQA has more COR and TR, with CR being the most difficult. GPT is better at answering. FVQA has a large number of OLR questions, but they are relatively easy. To further fine-tune ViFP on FVQA, more attention should be given to GL, FR and COR.

#### G. Visual Reasoning

ViFP is evaluated on Grok-4, Gemini-2.5, and GPT-4o. Table V and Fig. 5 show the reasoning accuracy and improve-

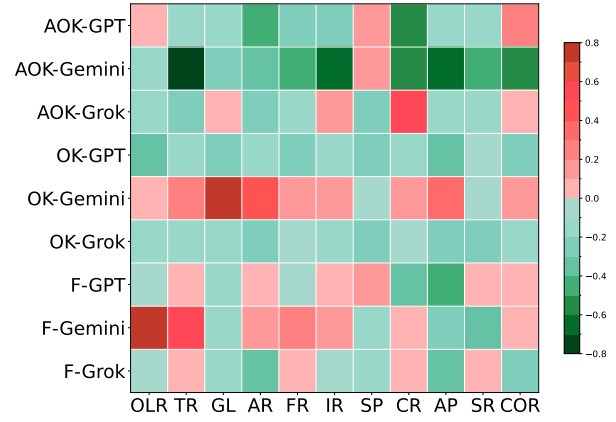


Fig. 5. Improvement of ViFP-base VLMs

ments on three real-world VQA datasets. Table 5 reveals that ViFP significantly enhances the reasoning accuracy of closed-source VLMs. As shown in Fig. 5, ViFP can help VLM to handle most types of questions, especially GPT and Gemini on A-OKVQA, GPT and Grok on OK-VQA, Grok on FVQA (green represents improvement, red represents decline).

The only exception is ViFP-based Gemini on OK-VQA and FVQA. This phenomenon occurs primarily because accuracy on open-ended VQA datasets is greatly influenced by the model's parameter scale and response preferences. The parameter scale of Gemini-2.5-flash is smaller than that of GPT-4o and Grok-4. Its logical reasoning ability is relatively weak, making it prone to over-interpretation or generating excessive irrelevant reasoning in multi-step reasoning processes. Although it generates many approximate answers, its accuracy decreases because they do not completely match the ground truth. In addition, when provided with longer reasoning cues, Gemini also tends to produce longer responses. We counted the number of instances in which the VLM's answer contained more than one word while the correct answer consisted of only one word. Gemini-2.5 had 1370 such instances, Grok-4 had 683, and GPT-4o had the fewest, with only 171. Therefore, if the number of words in the answer can be specified accurately, these VLMs, particularly Gemini-2.5, are likely to achieve significantly higher accuracy on open-ended VQA datasets.

Finally, we analyzed the incorrect answers in Gemini-2.5+ViFP and summarized them as follows:

- (1) Morphological disagreement and semantic granularity errors: such as Gemini-2.5+ViFP's answers being "vases" ( $A^*$ : vase) and "Kitchen island" ( $A^*$ : island);
- (2) Over-interpreted and speculation: such as the question is "Who leaves a toilet like this?" ( $A^*$ : man), the answer of Gemini-2.5 is "Everyone" and the answer of Gemini-2.5+ViFP is "Someone untidy", because "toilet... has its lid and seat up", ViFP helps VLM to focus the new clue: toilet seat, and the multi-step reasoning process is closer to the ground truth than direct answering. However, since the VLM is unaware that the ground truth is man/woman, it overinterprets as "untidy";
- (3) Category-level mismatches: such as the question "What type of plane is that?" ( $A^*$ : commercial), where Gemini-2.5+ViFP's answer is "Boeing 737-800";

TABLE VI  
ABLATION STUDY RESULTS ON A-OKVQA, “VoC-BASE” INDICATES THAT ALL ABLATION STUDIES TAKE THIS RESULT AS THE BASELINE.

Model	Acc	VoC	FP	TDFM
GPT-4o (VoC-base)	88.8	0	—	—
GPT-4o+Let’s think step by step	89.8	0.83	5	23
GPT-4o+LLaVA-CoT	89.3	0.36	11	34
GPT-4o+ViFP (QT=6)	85.1	-2.62	28	74
GPT-4o+ViFP (QT=9)	90.5	1.32	18	28
GPT-4o+ViFP (QT=11)	90.7	1.48	16	19
Gemini-2.5+ViFP (QT=11)	<b>92.0</b>	<b>2.47</b>	22	36

(4) Preference for internal knowledge: such as the question “What does this grow from?” ( $A^*$ : ground), where Gemini-2.5’s answer “From a bulb”.

#### H. Ablation Study

Ablation studies are conducted to verify the effectiveness of the components in ViFP. Moreover, VoC is introduced to intuitively show the contribution of the FP detection module.

1) *Impact of Question Type Granularity on Reasoning*: As shown in Table VI, we compare the accuracy under different  $QT$ s using GPT-4o. In the early stage, when the  $QT$ s were still coarse ( $QT = 6$ ), a significant proportion of questions were ambiguously classified, the  $Sq_i$  failed to provide effective reasoning guidance and thus negatively affected the reasoning accuracy. As classification became more refined ( $QT = 11$ ), the accuracy gradually improved, indicating that the VLM can arrive at the correct answer by refining its  $Sq_i$ .

2) *ViFP Compared to Generic CoT Method*: We further compare the reasoning chains generated by ViFP with generic CoT prompts. Table VI shows that the generic CoT prompts provide limited benefits to the VLM. Their chains lack specificity and are ineffective in guiding the VLM to focus on the key elements necessary for answering the question. When VLM does not know the explicit reasoning path, it tends to describe the image comprehensively by generating image captions, rather than trying to focus on the key points in the image according to the question, potentially resulting in a FP or accumulation of errors. In contrast, the reasoning chains generated by ViFP explicitly guide the VLM to focus on the key visual information in the images and offer the reasoning paths, significantly improving answer accuracy and reasoning reliability.

3) *Validating Reasoning Reliability with VoC*: VoC is calculated based on the results of direct reasoning and multi-step reasoning. Multi-step reasoning places greater demands on the VLM’s contextual understanding and cognitive abilities. Therefore, closed-source VLMs are used to compute VoC, FP and TDFM in order to better evaluate the improvement in reasoning reliability.

As  $QT$  is refined, the reliability of multi-step reasoning improves significantly. First, the number of TDFMs decreases steadily, indicating that errors caused by the reasoning chains produced by ViFP are being reduced. Second, the number of FPs decreases while the FP/TDFM ratio increases. This

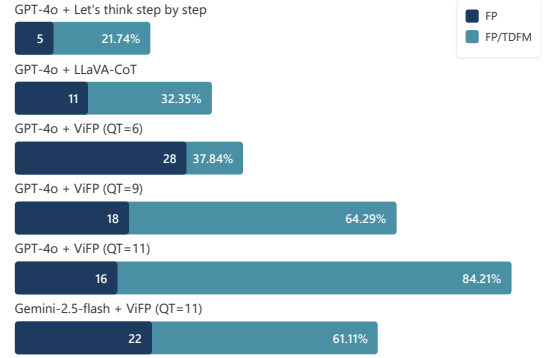


Fig. 6. The variation of FPs and FP/TDFM.

suggests that more TDFMs are converted into non-TDFMs, as more FPs are corrected to true positives. In addition, VoC usually increases with accuracy, but doesn’t always decrease as FP decreases. This is because FP only reflects the number of FPs that can be detected, can not fully account for all latent incorrect reasoning. However, with similar accuracy, a lower number of FPs indicates a higher VoC. This suggests that multi-step reasoning in this round has a higher reasoning reliability.

4) *Significance of negative VoC*: It is worth noting that when  $QT = 6$ , VoC is negative (-2.62). This is because the reasoning chains actually weaken the VLM’s reasoning ability, resulting in the generation of unreasonable paths. This observation is of great significance, as it quantitatively demonstrates that a poorly designed reasoning chain not only fails to help but also interferes with the VLM’s normal reasoning process, highlighting the necessity of refined question classification and reasoning chain optimization. As the  $QT$  and  $Sq_i$  become more refined, the VLM achieves improvements in reasoning accuracy and reliability simultaneously.

#### I. Case Study and Visualization of Accuracy Improvement Mechanisms

Based on the comparison with existing CoT methods, we summarize that ViFP mainly serves two functions. It improves VQA accuracy by providing effective and explicit reasoning chain, and enhances reasoning stability and reliability by correcting unreliable reasoning chains. Fig. 7 illustrates the two improvement instances.

## V. CONCLUSION

In this paper, we propose ViFP, which can be applied directly to VLMs with no need for additional training. ViFP enables VLMs to detect FPs independently. Unlike traditional cross-model verification methods, ViFP uncovers a broader range of potential FPs. Furthermore, ViFP introduces a visual reasoning optimization method based on feedback from FPs, which adjusts question types and reasoning chains. This guides the VLM towards more reliable reasoning paths and more accurate answers. We also introduce a novel metric called VoC to evaluate the value of FP correction in multi-step reasoning.





I1: Non-FP	Incorrect Reasoning by GPT-4o	ViFP-based Reasoning
 <p><b>Question:</b> How many bake pans were utilized?</p> <p><b>Answer:</b> A. one B. none C. <b>four</b> D. three</p>	<p><i>U: Answer the question and tell me the reason</i> A: <b>three</b>. The image shows a slice of layered <b>cake</b>, consisting of three distinct <b>layers</b>. Each layer likely required a separate bake <b>pan</b>, leading to the conclusion of 'three' bake pans used.</p> <p>pan → cake → layer → <b>D</b></p> <p><b>True Path</b> <b>False Answer</b></p>	<p><i>S1: Object Discovery</i> A: The main object to focus on is the number of layers in the cake.</p> <p><i>S2: Characteristic Description</i> A: The cake has <b>four layers</b>, which can be clearly identified from the image. The number of layers suggests that four separate <b>pans</b> might have been used for layered baking.</p> <p><i>Q: How many bake pans were utilized?</i> A: <b>four</b>. It can be observed from the image that the cake has <b>four layers</b>. Typically, each layer consists of a separately baked <b>cake sheet</b>, so it is reasonable to infer that four baking pans were used.</p> <p>pan → cake → layer → <b>C</b></p>
I2: FP	Inconsistent Reasoning by GPT-4o	ViFP-based Reasoning
 <p><b>Question:</b> What period of the day does this photo reflect?</p> <p><b>Answer:</b> A. noon B. morning C. dawn D. <b>afternoon</b></p>	<p><i>U: Answer the question and tell me the reason</i> A: <b>afternoon</b>. The <b>shadows</b> cast by the <b>building</b> indicate that the <b>sun</b> is positioned at an angle often seen during the afternoon, and the <b>sky's</b> brightness aligns with this period.</p> <p><i>S1: Object Discovery</i> A: I need to focus on the building, shadows, and sky.</p> <p><i>S2: Characteristic Description</i> A: The <b>building's shadow</b> is relatively short, and the <b>sky</b> is bright, indicating that the <b>sun</b> is positioned relatively high in the sky.</p> <p><i>Q: What period of the day does this photo reflect?</i> A: <b>noon</b>.</p> <p>sun → building → shadow → <b>A / D</b></p> <p><b>FP Path</b> <b>Inconsistent Answer</b></p> <p>sky</p>	<p><i>S1: Temporal Information Discovery</i> A: There is a clock on the tower that directly indicates the time.</p> <p><i>S2: Object Discovery</i> A: I should focus on the <b>clock</b> on the tower and the <b>lighting conditions</b>.</p> <p><i>S3: Characteristic Description</i> A: The clock is circular with a dark face, Roman numerals, and gold-colored hands. It shows the time as approximately <b>5:45</b>. The sunlight casts long shadows on the building, and the sky is still relatively bright, suggesting it is late afternoon rather than early morning.</p> <p><i>Q: What period of the day does this photo reflect?</i> A: <b>afternoon</b>. Given the <b>lighting conditions</b> and shadows, it's more consistent with <b>5:45 PM</b> rather than early morning, so the period is afternoon.</p> <p>clock → time → <b>A</b></p> <p>Lighting condition</p>

Fig. 7. Two instances of how ViFP works: In instance 1 (I1), ViFP guides the VLM to focus on more details in the image by providing an effective reasoning chain. In I2, ViFP corrects unreliable reasoning through FP detection, and guides VLM to focus on the key information: the "clock".

VoC evaluates both the accuracy of reasoning answers and the soundness of reasoning paths.

In future work, we plan to incorporate reinforcement learning into the false alarm detection process in order to better calculate the rationality score of inference paths and further strengthen ViFP's FP detection capabilities. This will provide more entry points for improving visual reasoning reliability.

## REFERENCES

- [1] J. Li, D. Li, S. Savarese, and S. Hoi, "BLIP-2: Bootstrapping Language-Image Pre-training with Frozen Image Encoders and Large Language Models," in *Proceedings of the 40th International Conference on Machine Learning*. PMLR, Jul. 2023, pp. 19 730–19 742, iSSN: 2640-3498. [Online]. Available: <https://proceedings.mlr.press/v202/li23q.html>
- [2] W. Hu, Y. Xu, Y. Li, W. Li, Z. Chen, and Z. Tu, "BLIVA: A Simple Multimodal LLM for Better Handling of Text-Rich Visual Questions," *Proceedings of the AAAI Conference on Artificial Intelligence*, vol. 38, no. 3, pp. 2256–2264, Mar. 2024, number: 3. [Online]. Available: <https://ojs.aaai.org/index.php/AAAI/article/view/27999>
- [3] P. Jian, D. Yu, and J. Zhang, "Large Language Models Know What is Key Visual Entity: An LLM-assisted Multimodal Retrieval for VQA," in *Proceedings of the 2024 Conference on Empirical Methods in Natural Language Processing*, Y. Al-Onaizan, M. Bansal, and Y.-N. Chen, Eds. Miami, Florida, USA: Association for Computational Linguistics, Nov. 2024, pp. 10939–10956. [Online]. Available: <https://aclanthology.org/2024.emnlp-main.613/>
- [4] Y. Yao, T. Yu, A. Zhang, C. Wang, J. Cui, H. Zhu, T. Cai, H. Li, W. Zhao, Z. He, Q. Chen, H. Zhou, Z. Zou, H. Zhang, S. Hu, Z. Zheng, J. Zhou, J. Cai, X. Han, G. Zeng, D. Li, Z. Liu, and M. Sun, "MiniCPM-V: A GPT-4V Level MLLM on Your Phone," Aug. 2024, arXiv:2408.01800 [cs]. [Online]. Available: <http://arxiv.org/abs/2408.01800>
- [5] M. Huang, Y. Liu, D. Liang, L. Jin, and X. Bai, "Mini-Monkey: Alleviating the Semantic Sawtooth Effect for Lightweight MLLMs via Complementary Image Pyramid," Oct. 2024, arXiv:2408.02034 [cs]. [Online]. Available: <http://arxiv.org/abs/2408.02034>
- [6] Y. Wang, N. Yang, L. Wang, and F. Wei, "Examining False Positives under Inference Scaling for Mathematical Reasoning," Feb. 2025, arXiv:2502.06217 [cs]. [Online]. Available: <http://arxiv.org/abs/2502.06217>
- [7] L. Luo, Y. Liu, R. Liu, S. Phatale, M. Guo, H. Lara, Y. Li, L. Shu, Y. Zhu, L. Meng, J. Sun, and A. Rastogi, "Improve Mathematical Reasoning in Language Models by Automated Process Supervision," Dec. 2024, arXiv:2406.06592 [cs]. [Online]. Available: <http://arxiv.org/abs/2406.06592>
- [8] A. Setlur, C. Nagpal, A. Fisch, X. Geng, J. Eisenstein, R. Agarwal, A. Agarwal, J. Berant, and A. Kumar, "Rewarding Progress: Scaling Automated Process Verifiers for LLM Reasoning," Oct. 2024, arXiv:2410.08146 [cs]. [Online]. Available: <http://arxiv.org/abs/2410.08146>
- [9] J. Wei, X. Wang, D. Schuurmans, M. Bosma, B. Ichter, F. Xia, E. Chi, Q. V. Le, and D. Zhou, "Chain-of-Thought Prompting Elicits Reasoning in Large Language Models," *Advances in Neural Information Processing Systems*, vol. 35, pp. 24 824–24 837, Dec. 2022. [Online]. Available: [https://proceedings.neurips.cc/paper\\_files/paper/2022/hash/9d5609613524ecf4f15af0f7b31abca4-Abstract-Conference.html?ref=https://githubhelp.com](https://proceedings.neurips.cc/paper_files/paper/2022/hash/9d5609613524ecf4f15af0f7b31abca4-Abstract-Conference.html?ref=https://githubhelp.com)
- [10] L. Trung, X. Zhang, Z. Jie, P. Sun, X. Jin, and H. Li, "ReFT: Reasoning with Reinforced Fine-Tuning," in *Proceedings of the 62nd Annual Meeting of the Association for Computational Linguistics (Volume 1: Long Papers)*. Bangkok, Thailand: Association for Computational Linguistics, 2024, pp. 7601–7614. [Online]. Available: <https://aclanthology.org/2024.acl-long.410>
- [11] H. Tan, Y. Ji, X. Hao, M. Lin, P. Wang, Z. Wang, and S. Zhang, "Reason-RFT: Reinforcement Fine-Tuning for Visual Reasoning," Mar. 2025, arXiv:2503.20752 [cs]. [Online]. Available: <http://arxiv.org/abs/2503.20752>
- [12] Z. Chen, Q. Zhou, Y. Shen, Y. Hong, Z. Sun, D. Gutfreund, and C. Gan, "Visual Chain-of-Thought Prompting for Knowledge-Based Visual Reasoning," *Proceedings of the AAAI Conference on Artificial Intelligence*, vol. 38, no. 2, pp. 1254–1262, Mar. 2024, number: 2. [Online]. Available: <https://ojs.aaai.org/index.php/AAAI/article/view/27888>
- [13] Z. Zhang, Y. Yao, A. Zhang, X. Tang, X. Ma, Z. He, Y. Wang, M. Gerstein, R. Wang, G. Liu, and H. Zhao, "Igniting Language

- Intelligence: The Hitchhiker's Guide from Chain-of-Thought Reasoning to Language Agents," *ACM Comput. Surv.*, vol. 57, no. 8, pp. 206:1–206:39, Mar. 2025. [Online]. Available: <https://dl.acm.org/doi/10.1145/3719341>
- [14] H. Shao, S. Qian, H. Xiao, G. Song, Z. Zong, L. Wang, Y. Liu, and H. Li, "Visual CoT: Advancing Multi-Modal Language Models with a Comprehensive Dataset and Benchmark for Chain-of-Thought Reasoning," *Advances in Neural Information Processing Systems*, vol. 37, pp. 8612–8642, Dec. 2024. [Online]. Available: [https://proceedings.neurips.cc/paper\\_files/paper/2024/hash/0ff38d72a2e0aa6dbe42de83a17b2223-Abstract-Datasets\\_and\\_Benchmarks\\_Track.html](https://proceedings.neurips.cc/paper_files/paper/2024/hash/0ff38d72a2e0aa6dbe42de83a17b2223-Abstract-Datasets_and_Benchmarks_Track.html)
- [15] G. Xu, P. Jin, H. Li, Y. Song, L. Sun, and L. Yuan, "LLaVA-CoT: Let Vision Language Models Reason Step-by-Step," Feb. 2025, arXiv:2411.10440 [cs]. [Online]. Available: <http://arxiv.org/abs/2411.10440>
- [16] J. Johnson, B. Hariharan, L. van der Maaten, L. Fei-Fei, C. Lawrence Zitnick, and R. Girshick, "CLEVR: A Diagnostic Dataset for Compositional Language and Elementary Visual Reasoning," 2017, pp. 2901–2910. [Online]. Available: [https://openaccess.thecvf.com/content\\_cvpr\\_2017/html/Johnson\\_CLEVR\\_A\\_Diagnostic\\_CVPR\\_2017\\_paper.html](https://openaccess.thecvf.com/content_cvpr_2017/html/Johnson_CLEVR_A_Diagnostic_CVPR_2017_paper.html)
- [17] "A review of emerging research directions in Abstract Visual Reasoning," *Information Fusion*, vol. 91, pp. 713–736, Mar. 2023, publisher: Elsevier. [Online]. Available: <https://www.sciencedirect.com/science/article/pii/S1566253522002214>
- [18] L. Shen, G. Chen, R. Shao, W. Guan, and L. Nie, "MoME: Mixture of Multimodal Experts for Generalist Multimodal Large Language Models," *Advances in Neural Information Processing Systems*, vol. 37, pp. 42 048–42 070, Dec. 2024. [Online]. Available: [https://proceedings.neurips.cc/paper\\_files/paper/2024/hash/4a3a14b9536806a0522930007c5512f7-Abstract-Conference.html](https://proceedings.neurips.cc/paper_files/paper/2024/hash/4a3a14b9536806a0522930007c5512f7-Abstract-Conference.html)
- [19] J. Wu, X. Hu, Y. Wang, B. Pang, and R. Soricut, "Omni-SMoLA: Boosting Generalist Multimodal Models with Soft Mixture of Low-Rank Experts," in *2024 IEEE/CVF Conference on Computer Vision and Pattern Recognition (CVPR)*. Seattle, WA, USA: IEEE, Jun. 2024, pp. 14 205–14 215. [Online]. Available: <https://ieeexplore.ieee.org/document/10656615/>
- [20] H. Bao, W. Wang, L. Dong, Q. Liu, O. K. Mohammed, K. Aggarwal, S. Som, S. Piao, and F. Wei, "VLMo: Unified Vision-Language Pre-Training with Mixture-of-Modality-Experts," *Advances in Neural Information Processing Systems*, vol. 35, pp. 32 897–32 912, Dec. 2022. [Online]. Available: [https://proceedings.neurips.cc/paper\\_files/paper/2022/hash/d46662aa53e78a62afd980a29e0c37ed-Abstract-Conference.html](https://proceedings.neurips.cc/paper_files/paper/2022/hash/d46662aa53e78a62afd980a29e0c37ed-Abstract-Conference.html)
- [21] X. Tan, X. Wang, Q. Liu, X. Xu, X. Yuan, and W. Zhang, "Paths-over-Graph: Knowledge Graph Empowered Large Language Model Reasoning," in *Proceedings of the ACM on Web Conference 2025*, ser. WWW '25. New York, NY, USA: Association for Computing Machinery, Apr. 2025, pp. 3505–3522. [Online]. Available: <https://doi.org/10.1145/3696410.3714892>
- [22] D. Hao, Q. Wang, L. Guo, J. Jiang, and J. Liu, "Self-Bootstrapped Visual-Language Model for Knowledge Selection and Question Answering," in *Proceedings of the 2024 Conference on Empirical Methods in Natural Language Processing*, Y. Al-Onaizan, M. Bansal, and Y.-N. Chen, Eds. Miami, Florida, USA: Association for Computational Linguistics, Nov. 2024, pp. 1857–1868. [Online]. Available: <https://aclanthology.org/2024.emnlp-main.110/>
- [23] H. Wen, H. Zhuang, H. Zamani, A. Hauptmann, and M. Bendersky, "Multimodal Reranking for Knowledge-Intensive Visual Question Answering," Jul. 2024, arXiv:2407.12277 [cs]. [Online]. Available: <http://arxiv.org/abs/2407.12277>
- [24] Z. Ma, S. Li, B. Sun, J. Cai, Z. Long, and F. Ma, "GeReA: Question-Aware Prompt Captions for Knowledge-based Visual Question Answering," Feb. 2024, arXiv:2402.02503 [cs]. [Online]. Available: <http://arxiv.org/abs/2402.02503>
- [25] Y. Deng, C. Ye, Z. Huang, M. D. Ma, Y. Kou, and W. Wang, "GraphVis: Boosting LLMs with Visual Knowledge Graph Integration," *Advances in Neural Information Processing Systems*, vol. 37, pp. 67 511–67 534, Dec. 2024. [Online]. Available: [https://proceedings.neurips.cc/paper\\_files/paper/2024/hash/7cb04f510593c9ba30da398f5e0a7e7b-Abstract-Conference.html](https://proceedings.neurips.cc/paper_files/paper/2024/hash/7cb04f510593c9ba30da398f5e0a7e7b-Abstract-Conference.html)
- [26] A. Salemi, J. Altmayer Pizzorno, and H. Zamani, "A Symmetric Dual Encoding Dense Retrieval Framework for Knowledge-Intensive Visual Question Answering," in *Proceedings of the 46th International ACM SIGIR Conference on Research and Development in Information Retrieval*, ser. SIGIR '23. New York, NY, USA: Association for Computing Machinery, Jul. 2023, pp. 110–120. [Online]. Available: <https://doi.org/10.1145/3539618.3591629>
- [27] M. Khademi, Z. Yang, F. Frujeri, and C. Zhu, "MM-Reasoner: A Multi-Modal Knowledge-Aware Framework for Knowledge-Based Visual Question Answering," in *Findings of the Association for Computational Linguistics: EMNLP 2023*, H. Bouamor, J. Pino, and K. Bali, Eds. Singapore: Association for Computational Linguistics, Dec. 2023, pp. 6571–6581. [Online]. Available: <https://aclanthology.org/2023.findings-emnlp.437/>
- [28] R. Cao and J. Jiang, "Knowledge Generation for Zero-shot Knowledge-based VQA," in *Findings of the Association for Computational Linguistics: EACL 2024*, Y. Graham and M. Purver, Eds. St. Julian's, Malta: Association for Computational Linguistics, Mar. 2024, pp. 533–549. [Online]. Available: <https://aclanthology.org/2024.findings-eacl.36>
- [29] Z. Yu, X. Ouyang, Z. Shao, M. Wang, and J. Yu, "Prophet: Prompting Large Language Models with Complementary Answer Heuristics for Knowledge-based Visual Question Answering," *IEEE Transactions on Pattern Analysis and Machine Intelligence*, pp. 1–12, 2025. [Online]. Available: <https://ieeexplore.ieee.org/document/10970423/>
- [30] Z. Dong, J. Yi, Z. Zheng, H. Han, X. Zheng, A. J. Wang, F. Liu, and L. Li, "Seeing is Not Reasoning: MVPBench for Graph-based Evaluation of Multi-path Visual Physical CoT," May 2025, arXiv:2505.24182 [cs]. [Online]. Available: <http://arxiv.org/abs/2505.24182>
- [31] S. Aldazharova, G. Issayeva, S. Maxutov, and N. Balta, "Assessing AI's problem solving in physics: Analyzing reasoning, false positives and negatives through the force concept inventory," *Contemporary Educational Technology*, vol. 16, no. 4, p. ep538, Nov. 2024, publisher: Bastas. [Online]. Available: <https://www.cedtech.net/article/assessing-ais-problem-solving-in-physics-analyzing-reasoning-false-positives-and-negatives-through-the-force-concept-inventory/>
- [32] D. Schwenk, A. Khandelwal, C. Clark, K. Marino, and R. Mottaghi, "A-OKVQA: A Benchmark for Visual Question Answering Using World Knowledge," in *Computer Vision – ECCV 2022*, S. Avidan, G. Brostow, M. Cissé, G. M. Farinella, and T. Hassner, Eds. Cham: Springer Nature Switzerland, 2022, pp. 146–162.
- [33] K. Marino, M. Rastegari, A. Farhadi, and R. Mottaghi, "OK-VQA: A Visual Question Answering Benchmark Requiring External Knowledge," 2019, pp. 3195–3204. [Online]. Available: [https://openaccess.thecvf.com/content\\_CVPR\\_2019/html/Marino\\_OK-VQA\\_A\\_Visual\\_Question\\_Answering\\_Benchmark\\_Requiring\\_External\\_Knowledge\\_CVPR\\_2019\\_paper.html](https://openaccess.thecvf.com/content_CVPR_2019/html/Marino_OK-VQA_A_Visual_Question_Answering_Benchmark_Requiring_External_Knowledge_CVPR_2019_paper.html)
- [34] P. Wang, Q. Wu, C. Shen, A. Dick, and A. van den Hengel, "FVQA: Fact-Based Visual Question Answering," *IEEE Transactions on Pattern Analysis and Machine Intelligence*, vol. 40, no. 10, pp. 2413–2427, Oct. 2018. [Online]. Available: <https://ieeexplore.ieee.org/abstract/document/8046084>
- [35] Y. Hu, H. Hua, Z. Yang, W. Shi, N. A. Smith, and J. Luo, "PromptCap: Prompt-Guided Task-Aware Image Captioning," Aug. 2023, arXiv:2211.09699 [cs]. [Online]. Available: <http://arxiv.org/abs/2211.09699>
- [36] Z. Chen, J. Chen, Y. Geng, J. Z. Pan, Z. Yuan, and H. Chen, "Zero-shot Visual Question Answering using Knowledge Graph," Oct. 2021, arXiv:2107.05348 [cs]. [Online]. Available: <http://arxiv.org/abs/2107.05348>